

# Department of Pharmacology

# Qualifying Examination (Part I)

August 2-4, 2016

[ALL EXAMS TAKE PLACE IN THE BASS CONFERENCE ROOM, 436 RRB](#)

Date	Time	Exam #
Tuesday, August 2 <sup>nd</sup>	9:00 am- 11:00 am	(Exam #1) –
	11:30 am – 1:30 pm	(Exam #2) –
	1:35 pm – 3:35 pm	(Exam #3) –
Wednesday, August 3 <sup>rd</sup>	9:00 am- 11:00 am	(Exam #4) –
	11:30 am – 1:30 pm	(Exam #5) –
	1:35 pm – 3:35 pm	(Exam #6) –
	3:40 pm – 5:40 pm	(Exam #7) –
Thursday, August 4 <sup>th</sup>	9:00 am- 11:00 am	(Exam #8) –
	11:30 am – 1:30 pm	(Exam #9) –
	1:30 pm – 2:15 pm (Committee Meets to determine results – Bass Conf. Rm.)	
	2:15 pm – 2:30 pm (Results given to students – 449 PRB, Pharm South Conf. Rm.) <b>ALL COMMITTEE MEMBERS TO BE PRESENT</b>	

Please remember that this is a closed-book examination. You must be prepared to answer 4 of the 7 questions. Although not necessary, you may prepare written answers, overhead figures, or any type of materials that you think might be useful in the presentation of your answers. You may bring such preparation materials with you to the examination. The oral examination itself will not extend beyond two hours.

If you have any questions regarding the examination, please contact **Joey Barnett**

**BEST WISHES FOR YOUR SUCCESSFUL COMPLETION OF THE EXAMINATION!**

Genetic association studies suggest that variations in the 5-hydroxytryptamine (5-HT; serotonin) transporter (5-HTT) gene are associated with susceptibility to psychiatric disorders such as anxiety or post-traumatic stress disorder. Individuals carrying high 5-HTT expressing gene variants display low amygdala reactivity to fearful stimuli.

The main structure in the brain responsible for fear memory is the amygdala. The interneurons in the amygdala, particularly parvalbumin-containing interneurons (PV), the main population of interneurons in the amygdala, play a critical role in fear memory.

Serotonin released from serotonergic axons during fear conditioning modulates the amygdala activity primarily through activation of local interneurons.

To further clarify the role of serotonin in modulating the conditioned fear response, the study used mice overexpressing the 5-HTT (5-HTTOE), an animal model of the human variation in the 5-HTT gene. Mice were tested in the conditioned fear paradigm, for cFos expression (cFos, an immediate early gene, is often used as an index of neuronal activation *in vivo*), and for the activity of parvalbumin-containing interneurons (PV) in amygdala slices.

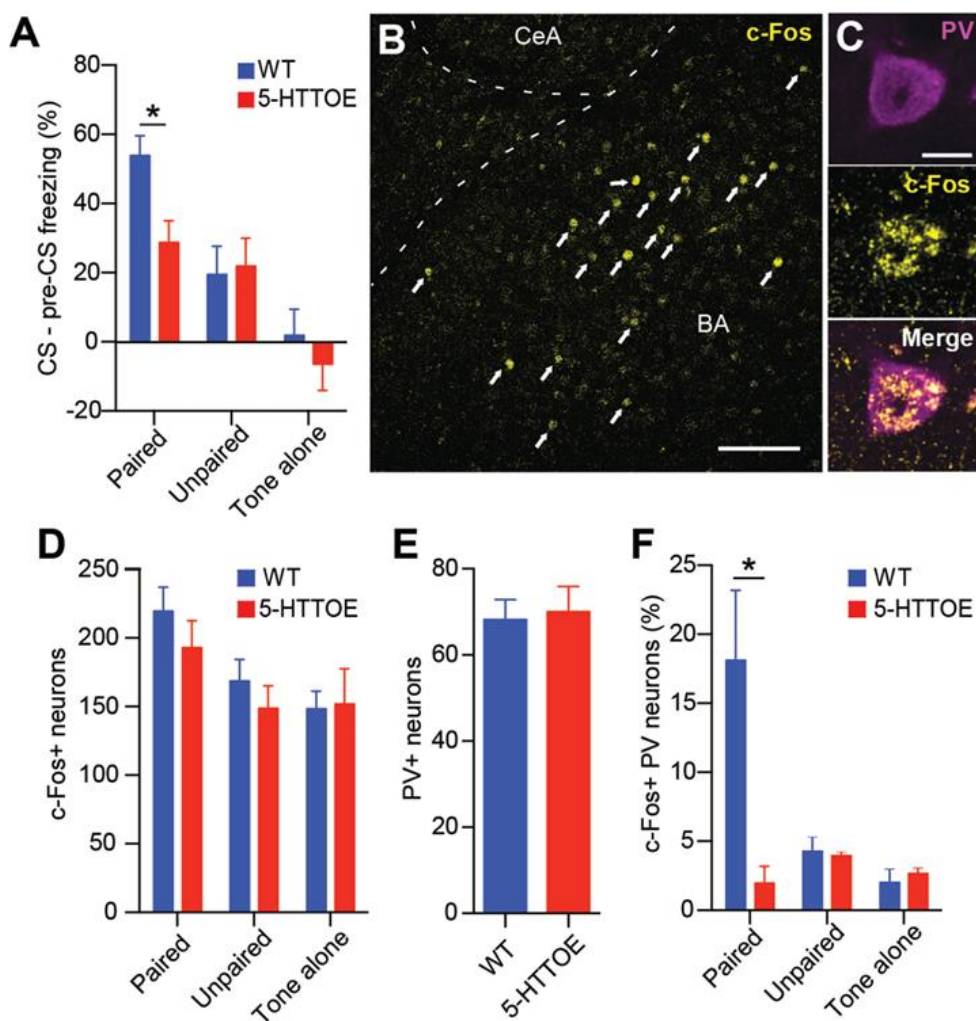


**Figure 1. Conditioned fear response and activation of PV interneurons in 5-HTTOE mice.** **A)** Freezing responses in 5-HTTOE mice as compared to wild type (WT). The data are expressed as the difference in freezing time in post- and pre-conditioning testing. CS – conditioned stimulus (tone). **B)** Representative c-Fos expression in the amygdala following the fear testing session detected by immunohistochemistry. Arrows indicate c-Fos+ neurons. Scale bar: 100  $\mu$ m. **C)** Immunoreactivity of a representative neuron for PV and c-Fos. Scale bar: 10  $\mu$ m. **D)** Overall numbers of c-Fos-positive (cFos+) neurons in the amygdala in WT and 5-HTTOE mice following the fear testing session. **E)** Overall numbers of PV neurons in the amygdala in WT and 5-HTTOE mice following the fear testing session. **F)** The numbers of c-Fos+/PV (as % of all PV neurons) in the amygdala of WT and 5-HTTOE in the paired condition. \*  $p < 0.05$ .

fear testing session. **F)** The numbers of c-Fos+/PV (as % of all PV neurons) in the amygdala of WT and 5-HTTOE in the paired condition. \*  $p < 0.05$ .

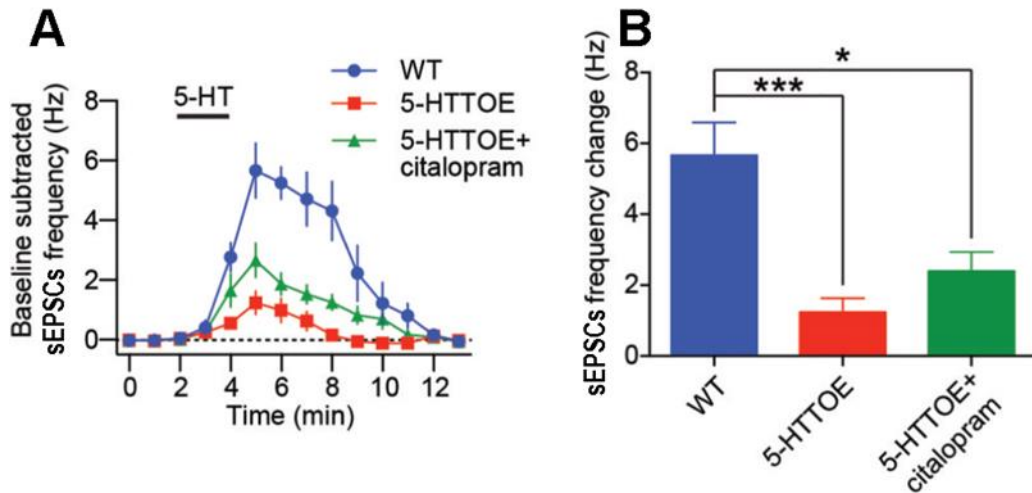


**Figure 2. Excitation of PV interneurons by 5-HT in the amygdala of WT and 5-HTTOE mice.** A) Time course of the effect of 5-HT (50  $\mu$ M) on sEPSCs frequency in WT and 5-HTTOE PVs. B) 5-HT-evoked frequency of sEPSCs in 5-HTTOE, compared to WT. Citalopram (1  $\mu$ M) was applied acutely to slices of 5-HTTOE mice. \*\*\*  $p < 0.001$ ; \*  $p < 0.05$ .

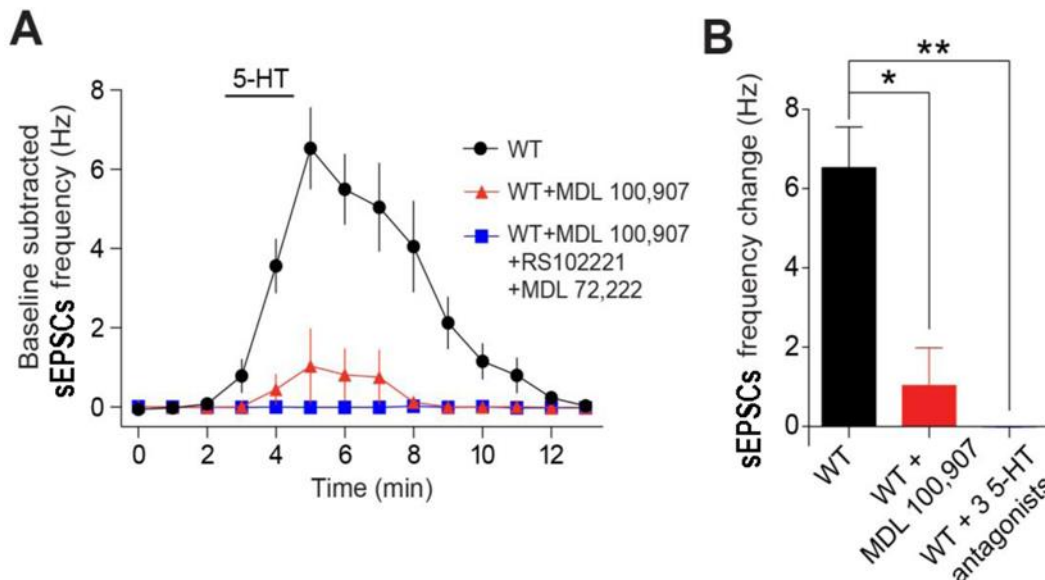


**Figure 3. 5-HT-induced activation of PV neurons in the amygdala in wild type mice.** A) Time course of the effect of bath application of 5-HT (50  $\mu$ M) on sEPSCs recorded from PVs of the amygdala in control conditions and in presence of MDL 100,907 (5-HT<sub>2A</sub> antagonist, 150 nM) or a combination of MDL 100,907 plus RS 102221 (5-HT<sub>2C</sub> antagonist, 1  $\mu$ M) and MDL 72,222 (5-HT<sub>3</sub> antagonist, 20  $\mu$ M). B) 5-HT-evoked frequency of sEPSCs in WT in the presence of antagonists\*  $p < 0.05$ ; \*\*  $p < 0.01$ .

**Questions:**

- 1. 5-HTTOE mice overexpress 5-HTT. How might the concentration of serotonin in the brain areas innervated by the serotonergic system be altered in these mice as compared to wild type?**

**How can you test this?**

- 2. What effect of 5-HTT overexpression do you see in these mice on the fear conditioning and activity of PV interneurons?**

**What is fear conditioning?**

- 3. What is the mechanism or action of citalopram? Which class of drugs does it belong to? What effect will it have when applied acutely to amygdala slices treated with 5-HT?**
- 4. What conclusions can you draw from Figs. 1, 2 and 3 as to the mechanisms underlying the behavioral/neuronal deficits in 5-HTTOE?**
- 5. Suggest a model of the serotonergic deficits in 5-HTTOE consistent with the data presented in Figs. 1-3.**

Organic cation transporter (OCT) 2, multidrug and toxin extrusion protein (MATE) 1, and MATE2K mediate the renal secretion of various cationic drugs and can serve as the loci of drug-drug interactions (DDI). To evaluate the cynomolgus monkey as a surrogate model for studying human organic cation transporters, monkey genes were stably transfected into human embryonic kidney (HEK) 293 cells (cultured in multiwell plates in monolayer) and their properties (substrate selectivity, time course, pH dependence, and kinetics) examined. Six known human cation transporter inhibitors, including pyrimethamine (PYR), showed generally similar IC<sub>50</sub> values against the monkey transporters (within sixfold) as judged by the *in vitro* inhibition of metformin (MFM) transport.

Intravenous and oral administration of MFM was also studied in two cynomolgus monkeys in the presence and absence of administration of PYR.

Background information, (not integral to the question, to aid understanding of the *in vitro* set-up)  
Methods (in vitro experiments): Briefly, HEK 293 cells were seeded into poly-D-lysine-coated 24-well plates at a density of  $0.5 \times 10^6$  cells per well. Two to three days after seeding, cells were grown to confluence, and uptake experiments were performed. Cells were washed twice with 1.5 ml Hanks' balanced salt solution (HBSS) prewarmed at 37°C. The uptake study was initiated by adding 0.2 ml of prewarmed standard buffer (HBSS containing 10mM HEPES, pH 7.4 for OCT2, and pH 8.4 for MATE1 and MATE2K, respectively) containing radiolabeled compounds (<sup>14</sup>C]MFM or others). At the end of the incubation period, the buffer was removed and the cells in each well were rinsed three times with 1 ml ice-cold HBSS (4°C). For a time course uptake study, the uptake of 2 mM [<sup>14</sup>C]MFM was terminated at specific times by aspirating and rinsing.

Also for your information, the estimated renal GFR of a cynomolgus monkey is approximately 3.0 ml/min/kg.

**Questions:**

**Interpret and briefly review the main features of the data for:**

- 1. The in vitro experiments**
- 2. The IV and oral in vivo experiments**
- 3. Suggest explanation(s) for any contradictions in the oral versus IV results. Design experiments to test your hypothesis.**

**(Note: Answers to Question 1 on the in vitro data should be brief, with more attention paid to Questions 2 and 3.)**

Representative data from the in vitro experiments on uptake of MFM into HEK293 cells stably expressing the transporters indicated.

FIGURE 1.

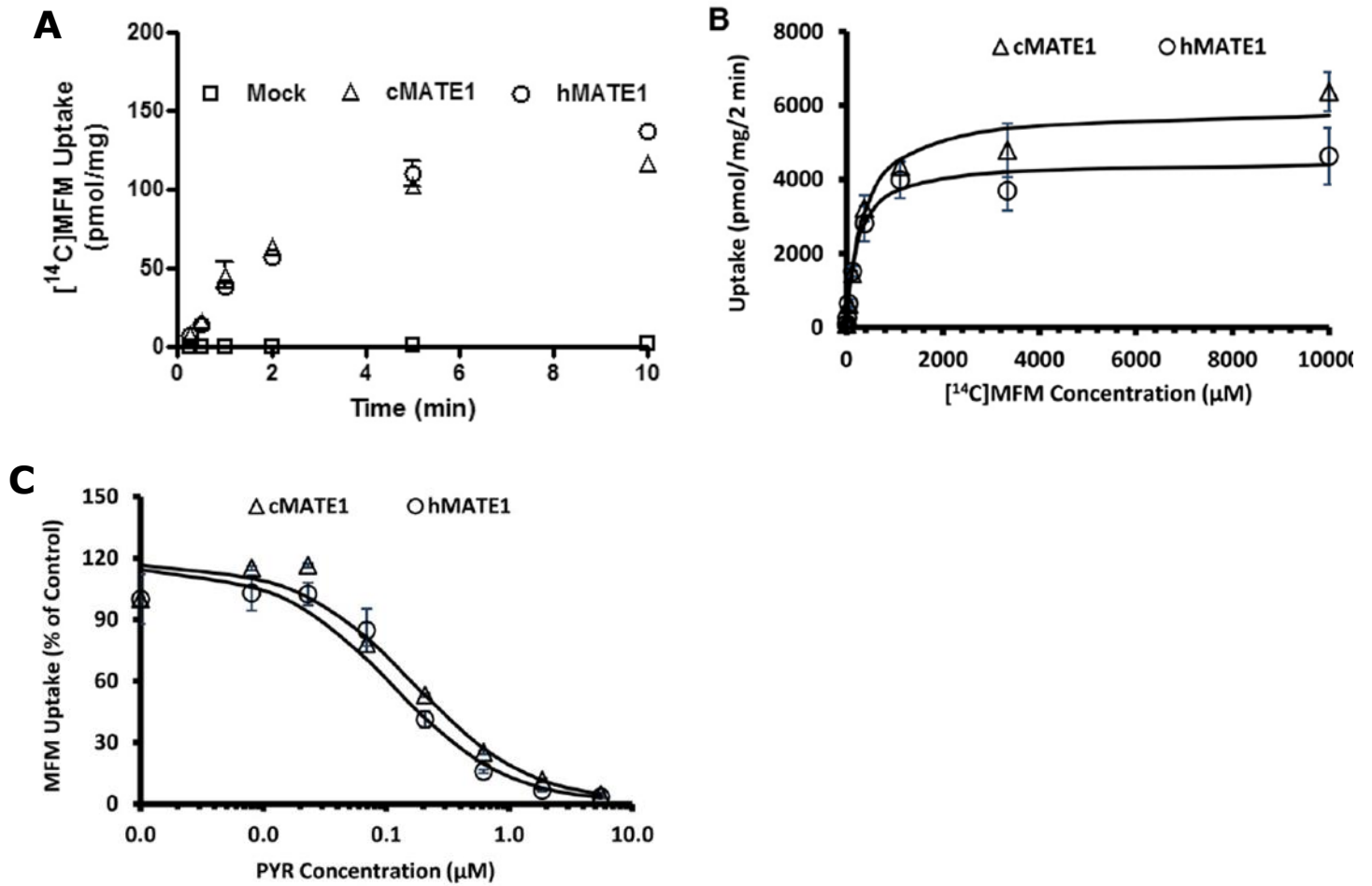


Fig. 1. Representative results using HEK293 cells stably transfected with MATE1 (cMATE1 = cynomolgus monkey; hMATE1 = human)

- A. Uptake of  $[^{14}\text{C}]\text{MFM}$  over 10 min.
- B. Comparison of uptake versus substrate concentration for monkey and human MATE1
- C. Inhibition curves for MFM uptake using PRY inhibitor for human and monkey proteins.

FIGURE 2.

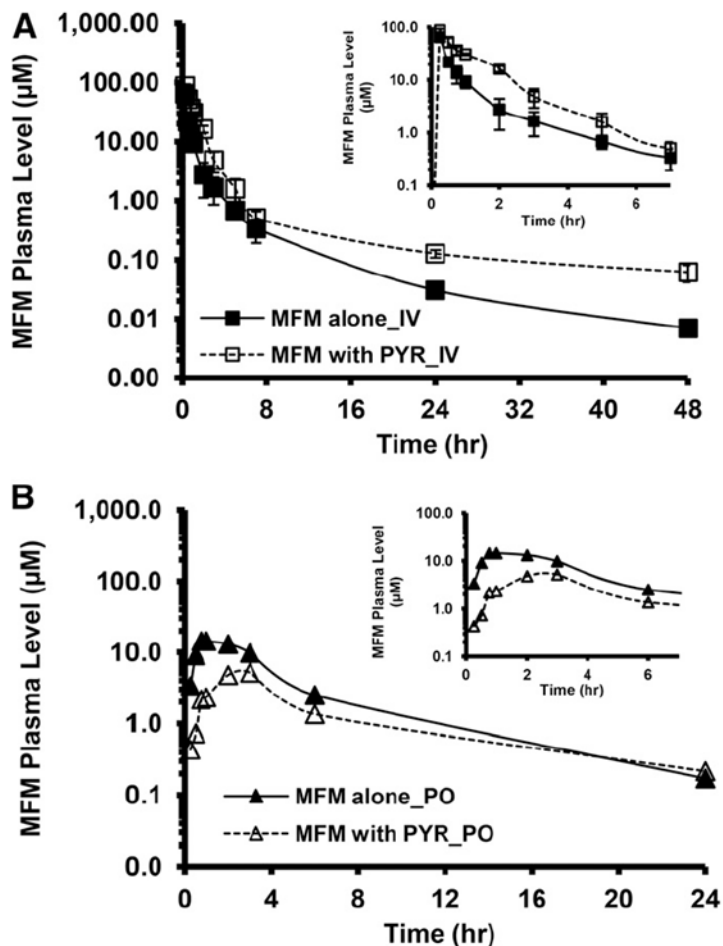


Fig. 2. Mean plasma concentrations of MFM [intravenous dose (A) and oral dose (B)] in cynomolgus monkeys after a single intravenous dose of 3.9 mg/kg MFM with and without PYR given as an intravenous dose (0.5 mg/kg; n = 3) and after a single oral dose of 8.6 mg/kg MFM with and without PYR given as an oral dose (2.5 mg/kg; n = 2). Insets depict the same data over a 7-hour period.

FIGURE 3.

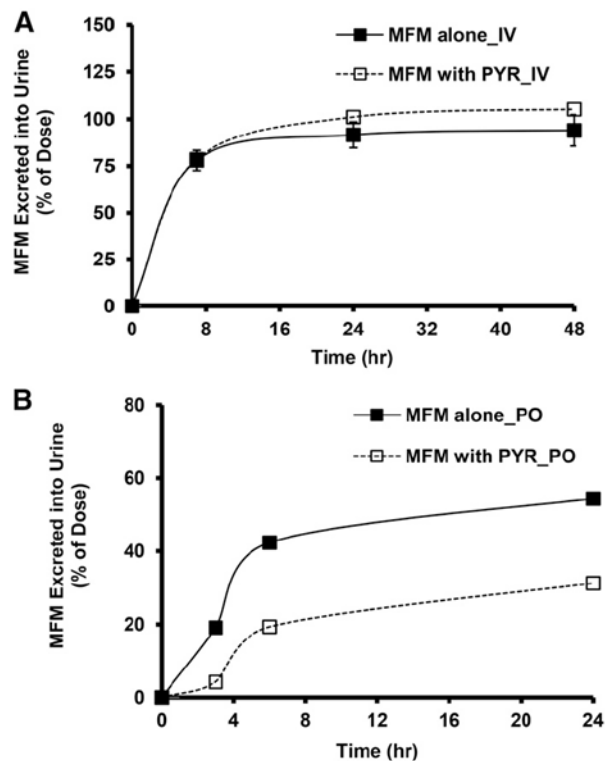


Fig. 3. Effects of PYR on urinary excretion of MFM after a single intravenous dose of MFM (3.9 mg/kg) alone or with PYR (0.5 mg/kg i.v.) (A) and after single oral dose of MFM (8.6 mg/kg) alone or with PYR (2.5 mg/kg by mouth) (B) in cynomolgus monkeys. The amount of MFM excreted in urine in monkeys was determined for the MFM alone (j) and PYR-treated (u) groups. PYR was dosed 1 hour ahead of MFM.

**Table of IV data**

Summary of pharmacokinetic parameters for MFM and PYR in cynomolgus monkeys ( $n = 3$ ) after a single intravenous dose of MFM (3.9 mg/kg) with and without an intravenous dose of PYR (0.5 mg/kg)

Analyte	Variable	MFM Alone	With PYR	Ratio (90% CI)
MFM	$AUC_{0-inf}$ ( $\mu\text{M}\cdot\text{h}$ )	$46.4 \pm 9.0$	$102 \pm 2.3^{**}$	2.23 (1.57–3.17)
	$V_{SS}$ (l/kg)	$0.98 \pm 0.16$	$0.88 \pm 0.21$	0.88 (0.45–1.73)
	$CL$ (ml/min/kg)	$11.2 \pm 2.4$	$5.0 \pm 0.1^*$	0.45 (0.32–0.64)
	% Urinary excretion of dose (0–48 hours)	$94.1 \pm 8.4$	105 (79.8 and 130) <sup>a</sup>	N.C.
	$CL_R$ (ml/min/kg)	$10.7 \pm 3.1$	5.3 (3.9 and 6.7) <sup>a</sup>	N.C.
	$T_{1/2}$ (hour)	$7.1 \pm 1.3$	$13.9 \pm 1.8^{**}$	1.98 (1.74–2.25)

Data are shown as mean  $\pm$  S.D. ( $n = 3$  animals). The pharmacokinetic parameters were determined as indicated under *Materials and Methods*. PYR was intravenously dosed 60 min before MFM.

<sup>a</sup>Cage malfunction prevented urine collection from one animal in the coadministration treatment group ( $N = 2$ ).

\* $P < 0.05$  and \*\* $P < 0.01$  compared with values for the in the absence of PYR; N.C., not calculated.

**Table of oral data**

Summary of pharmacokinetic parameters for MFM and PYR in cynomolgus monkeys ( $n = 2$ ) after a single oral dose of MFM (8.6 mg/kg) with and without an oral PYR dose (2.5 mg/kg)

Analyte	Variable	Animal #1		Animal #2		Average	
		MFM Alone	With PYR	MFM Alone	With PYR	MFM Alone	With PYR
MFM	$C_{max}$ ( $\mu\text{M}$ )	11.4	4.8	21.3	7.8	16.4	6.3
	$T_{max}$ (hour)	2.0	3.0	0.8	2.0	1.4	2.5
	$AUC_{0-24\text{hour}}$ ( $\mu\text{M}\cdot\text{h}$ )	62.6	24.0	67.2	34.4	64.9	29.2
	$AUC_{0-inf}$ ( $\mu\text{M}\cdot\text{h}$ )	63.9	25.6	67.6	35.6	65.7	30.6
	% Urinary excretion of dose (0–24 hours)	57.9	25.5	50.8	37.0	54.5	30.8
	$CL_R$ (ml/min/kg)	10.1	11.1	8.4	11.6	9.2	11.3
	$T_{1/2}$ (hour)	4.0	5.5	3.1	4.5	3.6	5.0

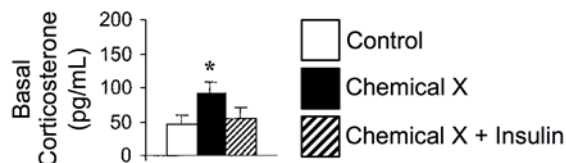
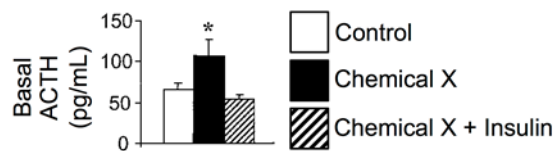
Data from individual animal are shown ( $n = 2$  animals). The pharmacokinetic parameters were determined as indicated under *Materials and Methods*. PYR was orally dosed 60 min before MFM.

You are using Chemical X to induce diabetes in an animal model, and make the following observations after several weeks of treatment of animals with Chemical X:

	Control	Chemical X	Chemical X + insulin
n	9	9	3
Body weight (g)	405.7 ± 7.0	304.2 ± 12.3	516.6 ± 8.8
Adrenal weight (mg)	25.3 ± 1.2	32.1 ± 1.0	32.0 ± 1.0
Relative adrenal weight (mg/kg body weight)	61.8 ± 3.2	107.5 ± 4.6	62.0 ± 1.9
Glucose (mg/dl)	121.3 ± 4.1	702.0 ± 48.2	110.9 ± 24.7

1. Does Chemical X treatment model Type 1 or Type 2 diabetes better? Provide rationale for your answer.

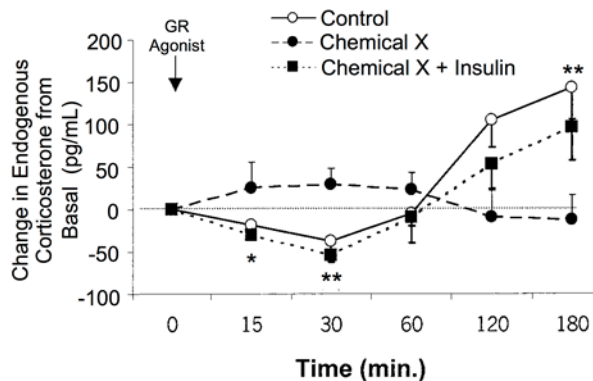
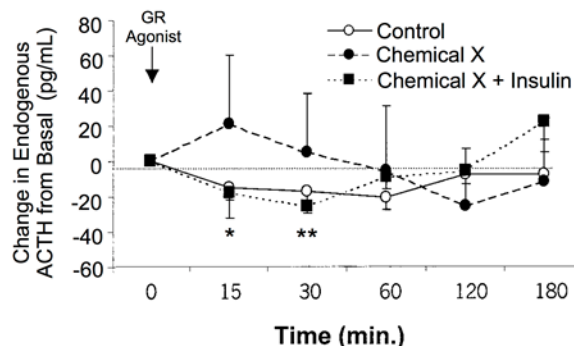
The data table in A. unexpectedly revealed adrenal hypertrophy after several weeks of Chemical X induction of diabetes. You measure basal levels of adrenocorticotrophic hormone (ACTH) and corticosterone levels in these animals after several weeks of Chemical X induction of diabetes, producing the data provided here. An asterisk indicates a significant difference compared to control.



2. Suggest a hypothesis explaining the adrenal hypertrophy.

Using Chemical X to induce diabetes in animals over several weeks, you then measure endogenous ACTH and corticosterone levels upon acute intravenous injection of a glucocorticoid receptor (GR) agonist. Asterisks indicate significant difference from basal; all other data points are not significantly different. Further, there are no significant differences between any “Control” vs. “Chemical X + Insulin” data points.

3. Based on the data provided here, develop a physiological hypothesis explaining the increase in basal corticosterone levels you observed in Part B.



Abnormal activation of c-Met in cancers correlates with poor prognosis. c-Met, also known as HGFR (hepatocyte growth factor receptor), is a receptor protein tyrosine kinase that can be activated by HGF. It has been shown that c-Met also can be activated upon the stimulation of epidermal growth factor (EGF) and several GPCR's including lysophosphatic acid (LPA) and thrombin (Thr) receptors.

The following experiments (Figures 1-4) were conducted to investigate the mechanisms underlying the transactivation of c-Met by EGF and GPCR's in the pancreatic carcinoma cell line, DAN-G. Several inhibitors were employed including AG1478 (an EGFR inhibitor), EGCG (Epigallocatechin gallate, a reducing agent), DPI (Diphenyleneiodonium chloride, an NADPH oxidase-specific inhibitor) and toxin B (an inhibitor for GTPases of the Rac, Rho, and Cdc42 families).

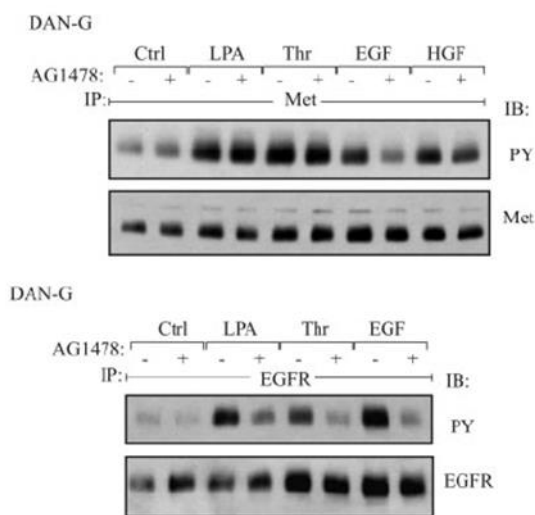


**Fig 1:** Activation of c-Met (top) and EGFR (bottom) in the presence of AG1478.

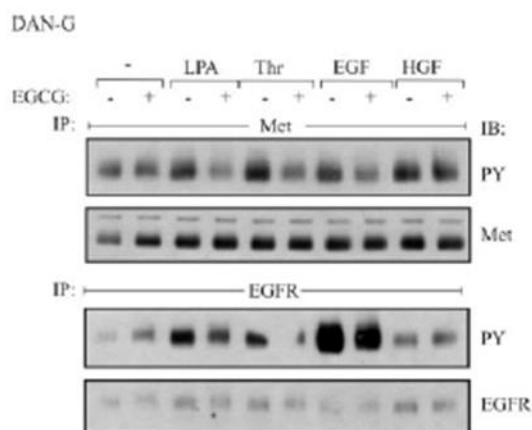


**Fig 2:** Activation of c-Met and EGFR in the presence of EGCG.

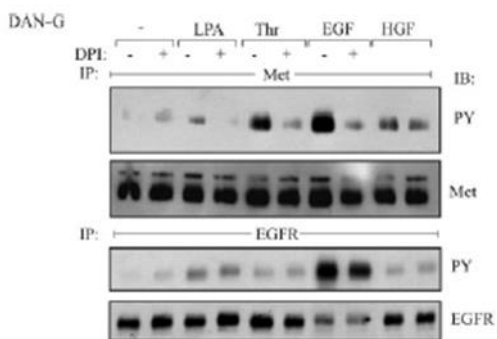


**Fig 3:** Activation of c-Met and EGFR in the presence of DPI.

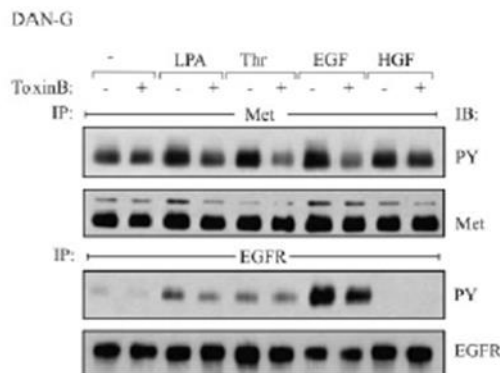


**Fig 4:** Activation of c-Met and EGFR in the presence of Toxin B.

**Questions:**

1. What are the key findings in each Figure?
2. Based on the findings, speculate how EGFR could be activated by LPA or Thr (using a diagram).
3. Based on the findings, propose how c-Met could be activated by LPA and EGF respectively (using a diagram).

Calmodulin (CaM) is an essential Ca binding protein that transduces Ca signals in a wide range of biological processes. CaM binds to larger proteins and functions as a Ca sensor for decoding Ca signals into downstream responses. In the heart, CaM regulates many ion channels such as the L-type Ca channel (Ca-dependent inhibition), Ca-activated K channels (Ca-dependent activation) and the RyR2 sarcoplasmic reticulum Ca release channel (Ca-independent inhibition). Humans have 3 CaM genes – *CALM1*, *CALM2*, *CALM3* – encoding the identical amino acid sequence that are all expressed in the heart muscle.

Genetic linkage studies have identified autosomal dominant CaM missense mutations in humans with severe ventricular arrhythmia and sudden cardiac death susceptibility, albeit with distinct clinical presentations ranging from stress-induced polymorphic ventricular tachycardia reminiscent of catecholaminergic polymorphic ventricular tachycardia (CPVT) over severe QT prolongation reminiscent of a long QT syndrome (LQTS) to idiopathic ventricular fibrillation (IVF).

A molecular autopsy identified two CaM mutations in a cohort of 50 children that died suddenly. In order to determine the underlying mechanism responsible for the sudden death cases, recombinant mutant CaMs were made and their effect on the cardiac action potential (AP) studied in mouse ventricular myocytes using current clamp. 6  $\mu\text{M}$  of WT, A103V mutant or D96V mutant CaM was added to the pipette solution and dialyzed into the cell via patch pipette. A train of four action potentials (1 Hz) was triggered by application of a 2-ms current injection 20 % above threshold. Resting potential and action potential (AP) duration measured at 50% and 90% repolarization (APD50 and APD90, respectively) were measured from the last paced AP for every cell. The incidence of early afterdepolarizations (EADs) was quantified for each cell during the pacing train. The incidence of delayed afterdepolarizations (DADs) and spontaneous beats triggered by DADs was calculated during the 45-s period after the pacing train. Results are shown Figure 1.

### Questions:

- 1. Describe the results of the AP measurements of Fig. 1. Formulate hypotheses for each CaM mutant on the underlying molecular mechanisms that could explain how mutant CaMs alter the cardiac action potential and cause EADs and DADs. Design experiments that will test your hypothesis.**
- 2. Based on the AP measurements, what clinical arrhythmia phenotype would you expect in patient carriers of A103V and D96V? Without having access to patients with the mutation (they are dead), how could you establish this using an alternative experimental approach?**

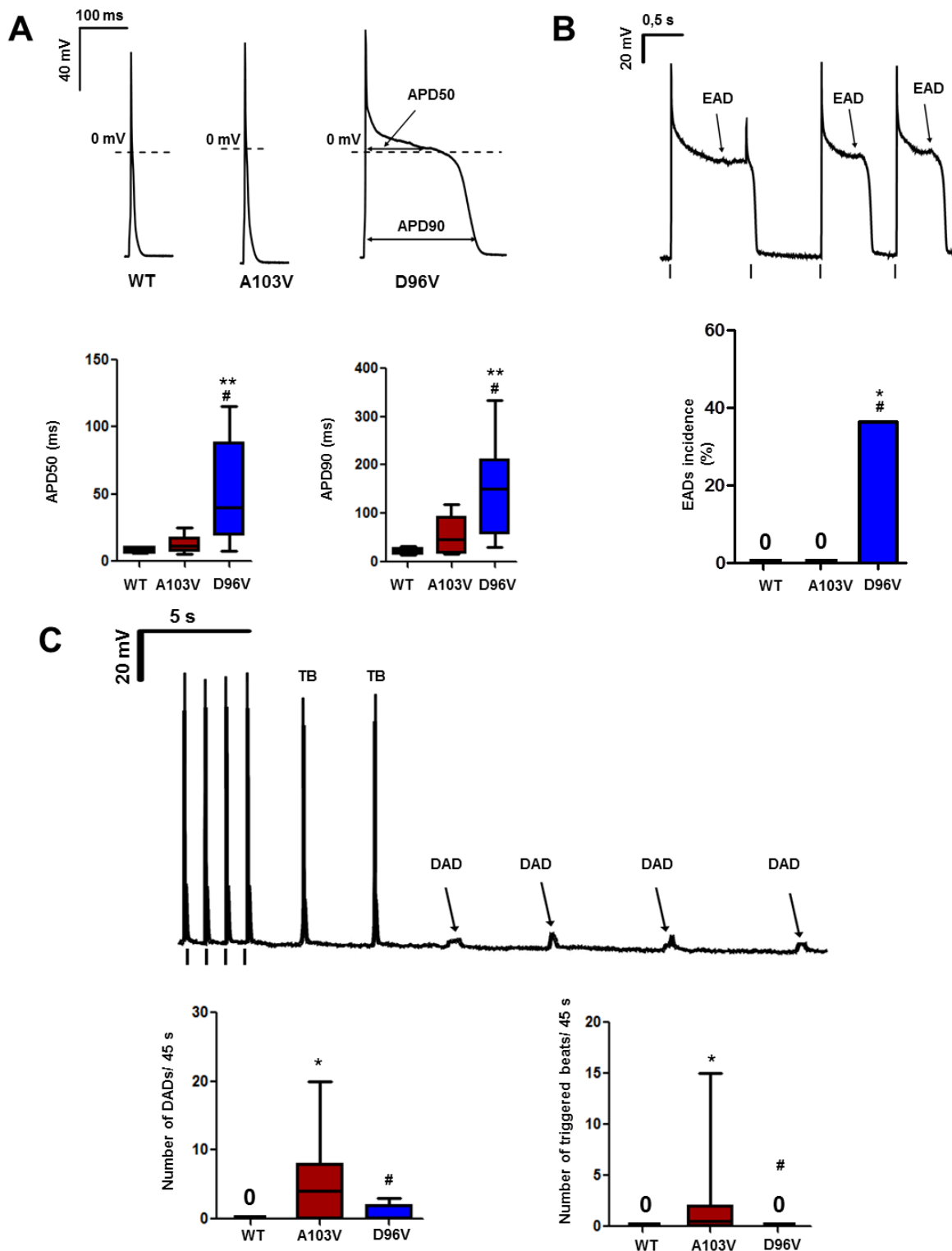


**Fig. 1. Measurement of cardiac action potentials in mouse ventricular cardiomyocytes.** **A.** Top panel: Representative examples of AP records for each experimental group. Bottom panel: Average APD measured at 50% (APD50, left) and 90% (APD90, right) of repolarization. **B.** Top panel: Representative example of prolonged APs with EADs recorded from a cardiomyocyte dialyzed with D96V-CaM. Bottom panel: Percentage of cardiomyocytes exhibiting EADs during the pacing train. **C.** Top panel: Representative examples of DADs and triggered beats recorded from a cardiomyocyte dialyzed with A103V-CaM. Bottom panel: Averaged number of DADs (left) and triggered beats (TB, right) during the first 45s after the pacing train in cardiomyocytes dialyzed with either WT or mutant CaMs. Data are mean  $\pm$  SD (WT-CaM n=7, A103V-CaM n=14 and D96V-CaM n=12 \* $p$ <0.05, \*\* $p$ <0.01 vs. WT-CaM; # $p$ <0.05vs. A103V-CaM).

Chloride transport by the renal tubule is critical for blood pressure (BP), acid-base, and potassium homeostasis. Chloride uptake from the urinary fluid is mediated by various apical transporters, whereas basolateral chloride exit is thought to be mediated by  $\text{ClC-Ka/K1}$  and  $\text{ClC-Kb/K2}$ , two chloride channels from the  $\text{ClC}$  family. Because inactivating mutations in  $\text{ClC-Kb/K2}$  cause Bartter syndrome, a disease that mimics the effects of the loop diuretic furosemide,  $\text{ClC-Kb/K2}$  is assumed to have a critical role in salt handling by the thick ascending limb. To dissect the role of this channel in detail, you generated a mouse model with a targeted disruption of the murine ortholog  $\text{ClC-K2}$ .

You test response to both furosemide and hydrochlorothiazide (HCTZ) and observe the following:

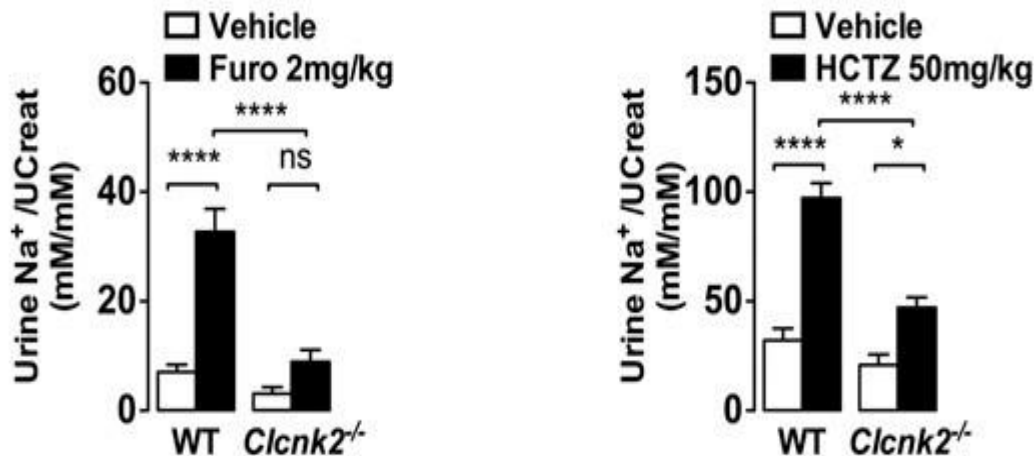


**Figure legend:** The effect of the pharmacological treatment using furosemide (furo) or HCTZ was compared between WT and knockout animals. Urine sodium was normalized to urine creatinine. Statistical analysis was performed using repeated measures ANOVA followed by Bonferroni posttest analysis. (N=5-10 for animals).

### Questions:

1. What is the site of action in the nephron for both furosemide and HCTZ?
2. Describe the results in the above figure. What do these data suggest about the localization and action of *Clcnk2* along the nephron?
3. How would you further test/confirm functional knockout of *Clcnk2* along the nephron?

Muscarinic M3D receptor, like many GPCRs, can signal via G proteins and arrestins. The authors created mutant receptor activated by CNO, as well as two biased mutants that selectively couple to Gq, but not arrestin (M3D-Gq) and arrestins, but not Gq (M3D-arr).

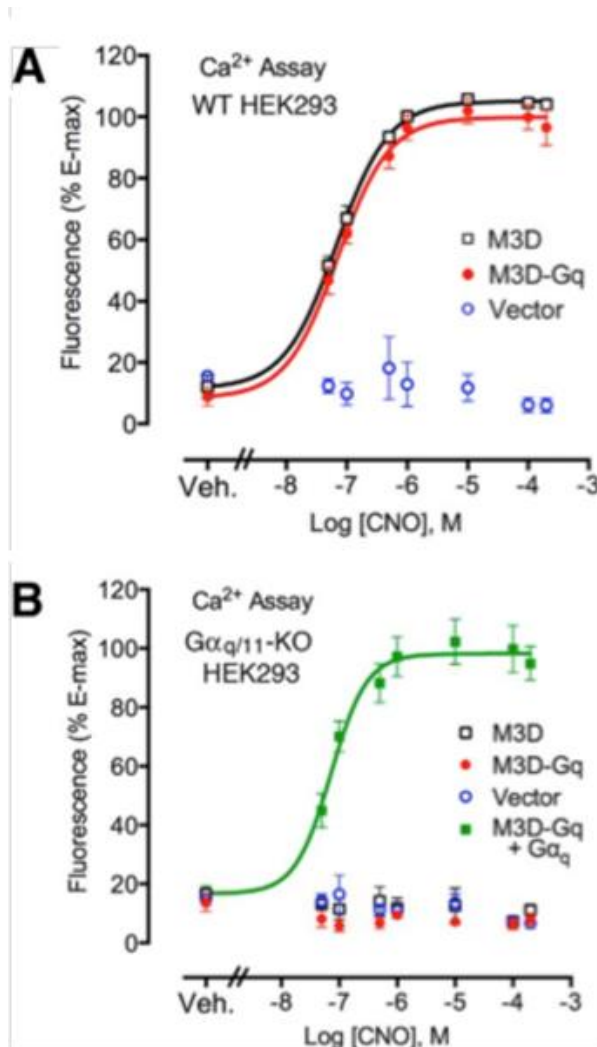


**Fig 1.** CNO treatment of M3D-Gq-expressing cultured cells leads to a G<sub>q/11</sub>-mediated increase in [Ca<sup>2+</sup>]<sub>i</sub>. WT HEK293 (A), or Gα<sub>q/11</sub>-deficient HEK293 (B) cells were transfected with the indicated constructs. CNO-induced increases in [Ca<sup>2+</sup>]<sub>i</sub> were determined using FLIPR. The data shown represent means ± S.E. from three independent experiments, each performed at least in triplicate. Gα<sub>q</sub>, human Gα<sub>q</sub> inserted into the pcDNA3.1 expression plasmid. Veh, vehicle.

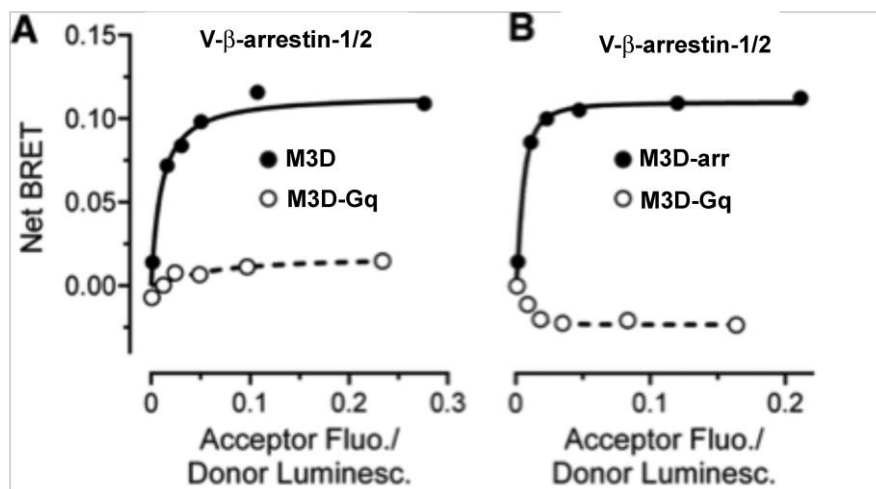


**Fig. 2.** BRET analysis of M3D-Gq/β-arrestin interactions. A,B HEK293 cells were co-transfected with luciferase (*Luc*)-tagged versions of M3D, M3D-arr, or M3D-Gq (luminescence donor) and β-arrestin-1 or -2 constructs carrying an N-terminal Venus (fluorescence acceptor) (*V*). BRET measurements were performed to monitor CNO-dependent M3D-Gq/β-arrestin interactions. A and B, BRET measurements were carried out in the presence of a fixed concentration of agonist CNO (20 μm). BRET signals are expressed as

net BRET values obtained by subtracting the net BRET ratio measured in the absence of CNO from the corresponding value obtained in its presence. Data are given as means ± S.E. from three experiments carried out in quadruplicate.

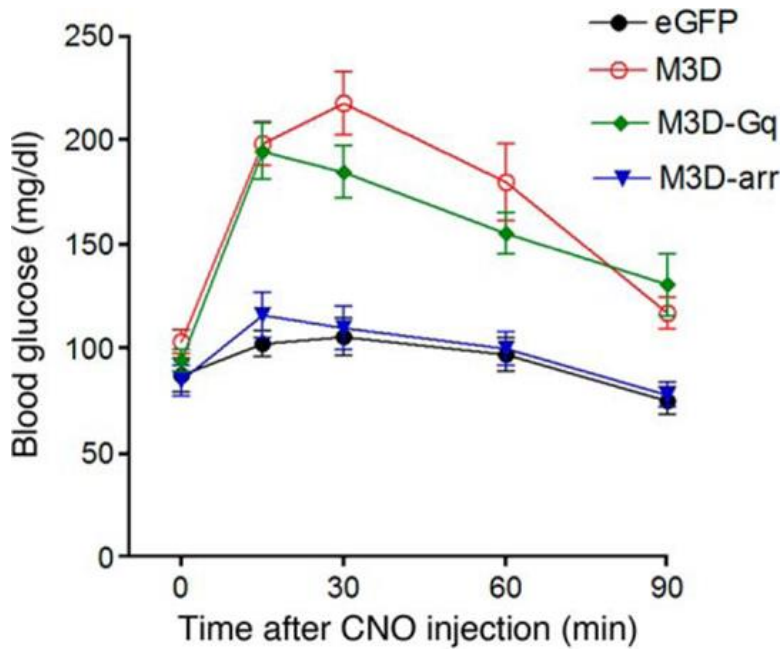


**Fig.3. Functional expression of M3D-Gq in mouse hepatocytes *in vivo*.** WT mice (8-week-old males) were injected i.v. with recombinant AAV viruses coding for M3D, M3D-Gq, or M3D-arr or with a control virus encoding eGFP. Two weeks later, mice were fasted overnight and then injected with CNO (10 mg/kg ip). The resulting changes in blood glucose levels were monitored over 90 min. Data are given as means  $\pm$  S.E. ( $n = 7-14$  mice per group).

### Questions

1. Why is panel B in Fig. 1 important? What does it show that panel A does not? Propose an additional experiment not shown here to test which G protein is involved.
2. What branch of M3D signaling regulates glucose level in mice?
3. Draw signaling pathways stimulated by M3D via G protein and arrestins. Which pathways does Fig. 3 exclude?
4. Describe at least one pathway M3D can activate via both G proteins and arrestins. Propose at least one experiment to test whether that particular pathway is involved in glucose regulation *in vivo*.